Journal of Colloid and Interface Science

In-situ synthesis of 3D ultra-small gold augmented graphene hybrid for highly sensitive electrochemical binding capability

Ayesha Taj[a,b], Ayesha Shaheen[a,b], Jie Xu[c], Pedro Estrela[d], Adnan Mujahid[e], Tayyaba Asim[f], M. Zubair Iqbal[g], Waheed S. Khan[a]**, and Sadia Z. Bajwa[a]*

[a]*National Institute for Biotechnology and Genetic Engineering (NIBGE), P.O. Box No.577, Jhang Road, Faisalabad, Pakistan*

[b]*Pakistan Institute of Engineering and Applied Sciences, Nilore, Islamabad, Pakistan*

[c]*Department of Industrial and Mechanical Engineering, College of Engineering, University of Illinois at Chicago, Chicago, US*

[d]*Centre of Biosensor Bioelectronics and Biodevices (C3Bio) and Department of Electronics and Electrical Engineering, University of Bath, Bath BA2 7AY, UK*

[e]*Institute of Chemistry, University of the Punjab, Quaid-i-Azam Campus, Lahore 54590, Pakistan*

[f]*Department of Environmental Science, Lahore College for Women University, Lahore 54590, Pakistan*

[f]*Department of Environmental Science, Lahore College for Women University, Lahore 54590, Pakistan*

[g]*Department of Materials Engineering, College of Materials and Textiles, Zhejiang Sci-Tech University, No.2 Road of Xiasha, Hangzhou, 310018. PR China*

Corresponding Authors; *Dr Sadia Z. Bajwa Email:sadya2002pk@yahoo.co.uk, sadia.zafar.bajwa@nibge.org; Tel: +92-41-9201404 Fax: +92-41-2651472; **Dr Waheed S. Khan Email: waheedskhan@yahoo.com, Tel: +92-41-2553519 Fax: +92-41-9201404

Abstract:

The fascinating properties of graphene can be augmented with other nanomaterials to generate hybrids to design innovative applications. Contrary to the conventional methodologies, we showed a novel yet simple, *in-situ*, biological approach which allowed for the effective growth of gold nanostructures on graphene surfaces (3D Au NS@GO). The morphology of the obtained hybrid consisted of sheets of graphene, anchoring uniform dispersion of ultra-small gold nanostructures of about 2-8 nm diameter. Surface plasmon resonance at 380 nm confirmed the nano-regimen of the hybrid. Fourier transform infrared spectroscopy indicated the utilization of amine spacers to host gold ions leading to nucleation and growth. The exceptional positive surface potential of 55 mV suggest that the hybrid as an ideal support for electrocatalysis. Ultimately, the hybrid was found to be an efficient receptor material for electrochemical performance towards the binding of uric acid which is an important biomolecule of human metabolism. The designed material enabled the detection of uric acid concentrations as low as 30 nM. This synthesis strategy is highly suitable to design new hybrid materials with interesting morphology and outstanding properties for the identification of clinically relevant biomolecules.

Keywords: Hybrid; graphene oxide; gold nanostructures; facile growth; electrochemical biosensor; cyclic voltammetry; biomolecules

1. Introduction

Hybrid nanostructures consist of two or more nanoscale functional components, where each one contributes its individual properties in synergy with the others, leading to interesting and diverse applications in various fields such as device fabrication, diagnostic, medicine, and energy conversion, *etc*. [1-2]. Their performance is highly dependent on the nature and properties of the individual components, including their size, shape, morphology, orientation, and distribution [3]. However, it imparts technical challenges to augment nanomaterials of different genre in three-dimensional (3D) hybrids to fabricate advanced multifunctional structures. Nanotechnology has burgeoned providing a plethora of options in this respect to furnish versatile hybrid nanomaterials [4-6]. Among those, the use of graphene as one of the hybrid components is of particular interest. Graphene is a two-dimensional monolayer of carbon honeycomb which yields a wealth of new enthralling properties such as extremely high electron mobility and, conductivity, extraordinary stiffness, and elasticity. Graphene can be functionalized in various ways to tailor nanomaterials with new catalytic, optical, electronic, thermal, and mechanical properties [7-9].

Conventionally, graphene hybrids are not highly dispersed with uniform morphology, impeding their useful applications. Most of the published reports on the preparation of graphene/metal hybrid materials utilize chemical methods to anchor the metallic nanoparticles to the graphene surface or require the use of organic solvents such as methanol and tetrahydrofuran, *etc.* [10-12]. Biosynthesis routes have received major attention by researchers because these enable the synthesis of large quantities of nanoparticles with well-defined size and outstanding

morphology [13]. Therefore, we can use the strength of green methods based on plant extracts, as an the inexpensive platform to generate efficient materials with the desired properties [13, 14]. In these methods multifunctional nanostructures can be prepared, where the characteristics of the nanomaterials are influenced by the source and nature of the extract [5, 15-17]. The environmentally benign biological reduction of precursor solution is a quite quick process and can be easily conducted at room temperature [9-10, 18]. Moreover, biomolecules present in the plant extracts may be used to synthesize different nanomaterials in a single step process of green synthesis [19].

In this paper, we present the development and characterization of a hybrid where, gold nanostructures are grown and ameliorated over graphene sheets using a simple, one step synthesis method in aqueous media. Gold is chosen for its traditional but unique optical and surface properties producing attractive applications ranging from catalysis, biomedical applications, to energy storage [1, 3]. We show that graphene oxide surfaces can be functionalized with amine groups to host the gold ions. These centres may act as the anchor for the nucleation and growth of gold nanostructures. We have exploited the potential of a medicinal plant, *i.e. Caryota mitis*. It is a multi-stemmed, clustering, evergreen plant which yields pure flavonoids quercetin-3-O-β-D-glucoside and rutin, and some methanolic compounds that exhibit strong antioxidant activity [20]. These compounds may act as reducing as well as stabilizing agents during the synthesis of nanostructures over graphene surfaces.

We anticipated the potential application of the prepared hybrid as a substrate for the electrochemical detection of biomolecules. In this respect, we selected uric acid (UA) which is

an important clinical analyte. It is used in many cellular responses, to treat and prevent many pathological disorders. It is a waste product of purine metabolism in the human body [21]. Purine is a double ring compound present in DNA and their normal levels in urinary excretion and blood serum are about 250-520 μM and 1.49-4.46 mM, respectively. The level of uric acid is also related to several disorders such as gout, hypertension, obesity, diabetes, high cholesterol, and heart diseases [22-25]. There are some conventional techniques which have been developed to determine the presence of uric acid, including enzymatic based assay [26], high performance liquid chromatography [27], capillary electrophoresis [28]. These methods are cumbersome, time consuming, and technically challenging [10]. In comparison, electrochemical methods are preferred over these conventional methods due to their inherent simplicity, rapidity, and sensitivity.

In the present study, we report an environmentally friendly, cost-efficient, and single step method to synthesize three-dimensional graphene hybrid augmented with ultra-small gold nanomaterials. This is the first report describing the *in-situ* growth of hybrid by using *Caryota mitis* extracts and then revealing its outstanding morphology and binding properties to recognize uric acid. The morphology is investigated by scanning electron microscopy (SEM), transmission electron microscopy (TEM) and atomic force microscopy (AFM), whereas, dynamic light scattering (DLS) and Fourier transform infrared spectroscopy (FTIR) experiments were performed for elucidating the structural and functional analyses. Cyclic voltammetry (CV) studies were performed to explore the electrochemical activities towards the binding of biomolecules. The designed material exhibited extraordinary electrochemical signals in the

presence of uric acid. This study opens up new avenues of designing versatile applications where the practical potential of such materials can be demonstrated for clinical diagnostics.

2. Materials and methods

All chemicals/reagents used in this work were either of analytical or highest procured grade, and these were utilized as-received. Graphene was obtained from the Shenzhen Nanotech Port. Co. Ltd (China). *Caryota mitis* flowers were taken from the Botanical Gardens of Agriculture University Faisalabad, Pakistan.

2.1. Preparation of three-dimensional gold nanostructures reinforced graphene oxide hybrid (3D Au NS@GO)

2.1.1 Preparation of Caryota mitis extract

For this purpose, flowers of *Caryota mitis* plants were collected from the botanical garden. These were dried under sunlight for 2-3 days, and then ground in a pestle mortar till a very fine dry powder was obtained. About 10 g powder was suspended in 80 mL of ultra-pure deionized water and then refluxed with continuous stirring for about 2 hours. The resultant mixture was allowed to cool down to ambient temperature. The as-prepared extract was further centrifuged at 8,000 rotations per minutes (RPM) for 20 minutes to remove the solid residues, followed by its filtering through Whatman filter paper (grade 1) possessing pore size 11 µm, to obtain a clear and transparent extract. Finally, the sample was stored at 2 °C to prevent the growth of microorganism for further use.

2.1.2 Surface functionalization of graphene oxide

To functionalize the graphene oxide this, 0.015 g of GO was suspended in polyethyleneimine (PEI) (1 % w/w solution in methanol). This suspension was sonication for 1.5 hours and maintained at room temperature. Later, the mixture was isolated by centrifugation (10 minutes; 4000 RPM; 25 °C) and the supernatant having excessive PEI was discarded. The obtained PEI wrapped graphene was re-suspended in 35 mL of methanol and sonicated till a stable dispersion was obtained.

2.1.3 Preparation of 3D Au NS@GO hybrid

A precursor solution of hydrogen tetrachloroaurate ($HAuCl_4$; 0.1 M) was prepared in 10 mL of methanol and then added to the PEI functionalized GO colloid, with vigorous stirring using a magnetic hot stirrer. After 30 minutes, the freshly prepared extract of *Caryota mitis* (10 mL) was added to the above reaction mixture and stirred further for almost 10 minutes. Afterwards, the suspension was centrifuged at 4000 RPM for 15 minutes and a pellet (3 mg) was obtained. The pellet was washed thoroughly with methanol and water solution (70:30). The process of centrifugation and washing was repeated several times, under the same conditions. The final hybrid material was dried at 50 °C under vacuum for 24 hours and it is referred as 3D Au NS@GO hybrid.

2.2 Characterization methods

The morphology was studied by field emission scanning electron microscopy (FESEM; JEOL, JSM-7500F), transmission electron microscopy (TEM; JEOL, JSM-1010) and atomic force microscopy (AFM; SHIMADDZU WET-SPM 9600 Japan).

To obtain information about the functionalities, we investigated the Fourier transform infrared (FTIR) profiles of the hybrids by using the attenuated total reflection (ATR) mode of Perkin Elmer system 2000. For this purpose, 5 mg each of 3 samples, at different level of synthesis were drawn *i.e.*, dispersion of GO in PEI and 3D Au NS@GO hybrid. Further, triplicate of each sample was taken and the averages of 10 scans of each sample were evaluated for each spectrum (0.005 m^{-1} spectral resolution). Optical characteristics were explored by UV-Vis spectroscopy and three independent experiments were performed for each sample (1 mg mL^{-1}). To investigate surface charge, zeta potential studies were carried out using a Zeta Sizer Nano Series (Malvern) instrument. For these studies, suspensions of graphene and PEI, and hybrid were first submitted to sonication to obtain homogeneous dispersions and then potentials were obtained.

2.3 Preparation of sensors

Prior to all experiments, glassy carbon electrodes (GCEs) were polished by alumina slurries (1.0, 0.3 and 0.05 μM) for 1 minute each, later cleaning copiously with ethanol and deionized water, to remove inorganic and organic impurities. In order to remove adsorbed contaminants, the electrodes were subjected to ten cycles in supporting media between -0.2 to 1 V *vs*. Ag/AgCl at a scan rate of 0.1 Vs^{-1}. To prepare the sensor, 0.5 mg of hybrid suspension was prepared in 1 mL deionized water. Out of this suspension, 10 μL were drop-casted on electrodes and dried in an oven at 60 °C for 10 minutes. The layers were then strengthened with 2 μL of the 5 % nafion and all the devices were dried at room temperature for 24 hours. To perform the control experiments, all procedures were followed, in the same way but excluding the addition of

the hybrid. Herein, 10 μL (0.5 mg mL^{-1}) each of graphene and gold nanostructures (Au NS) dispersions were coated to obtain graphene-modified and Au NS-modified electrodes, respectively.

2.4 Sensor studies

The electrochemical signals were recorded by using cyclic voltammetry (CV) technique. For this purpose, measurements were carried with a Potentiostate/Galvanostate (PGSTAT; Autolab) with a conventional system comprising of three electrodes; a glassy carbon electrode which was modified with hybrid (working electrode), a glassy carbon rod (counter electrode) and a Ag/AgCl electrode (reference electrode). These were placed in 25 mL of sodium phosphate monohydrate solution (background electrolyte; 50 mM) to conduct all the electrochemical experiments. Before each measurement, purging of the medium solution was carried out with nitrogen gas (99 %; for 5 minutes). All CV scans were recorded within potential range -0.2 to 1 V and at a scan rate of 50 mVs^{-1} (with the exception of the study of the influence of scan rate).

3 Results and discussion

3.1 Characterization of materials

3.1.1 Design mechanism of hybrid

In the present study, the gold nanostructures were immobilized on the amine functionalized graphene by a facile and *in-situ* method and following a biological induced reaction. Hence, the formation of hybrid involves mainly two steps; functionalization of GO, then nucleation and growth of gold structures. These two factors primarily drive the

nanostructures size and their distribution. GO is demonstrated as a substrate where, it can host nucleation centers for the growth of nanostructures. We propose the plausible formation mechanism and in this respect, Supplementary information (SI. 1) illustrates the necessary steps involved in the development of hybrid materials. In a typical experiment, firstly, amine groups were functionalized on graphene surface to generate reaction centers and to host structures growth over it (SI. 1; first step). Further, it was assumed that with the addition of precursor gold ions the nucleation of gold nanostructures at GO surfaces takes place which is mainly governed by the presence of amine groups contributing to an overall negatively charged surface. In fact, the gold ions coordinate with amine groups and lead to the formation of complexes (SI. 1; second step). Although, it is not possible to determine the extent of complexation, it is supposed that the amine functional groups are responsible for the attachment of freely moving gold ions. Next, plant extract was added which acted both as the reducing and capping agent, enabling and directing the growth of gold nanostructures at the graphene surface (Figure SI 1; third step). The use of biological extract has its own merits due to the presence of fairly high amounts of different biomolecules, such as sugars, amino acids, proteins, starch, antioxidants, enzymes, and many other metabolites as well as high levels of poly-phenols (Flavonoids) [30]. These compounds bear an abundance of hydroxyl (OH) groups which can act as reducing agents credibly involved in the biological reaction. This proposed biologically induced reduction converts Au^{+} ions into metallic Au^{o} nanostructures in the presence of these metabolites and redox enzymes [1, 31, 32]. The scheme depicted in Fig. 1 illustrates the steps proposed in the above discussion. Finally, the protein released from the plant extract may combine with the gold nanoparticles and stabilizes the final product [18].

3.1.2 Morphology and structural investigation of 3D Au NS@GO hybrid

The size, texture, and surface of the hybrid were studied by field emission scanning electron microscopy (FESEM). The obtained images are shown in Fig. 2 (A-C). A typical GO morphology, where translucent sheets are making an interconnected network and inherent wrinkles and folds of GO can be clearly observed (Fig. 2A). However, in the case of hybrid, it can be seen that the graphene skeleton is fully and uniformly covered by the network of Au nanostructures (2-8 nm) (Fig. 2B). Further the wrinkles and ripples were still observed, suggesting flexible structure and intact sheet morphology with high density loading of the nanostructures. Generally, the decoration of the nanomaterials is not uniform on the GO sheets owing to polydispersity of the surface active sites [33]. However, contrary to the previously reported bio extract methods for the synthesis of metallic structures, our method furnished a homogeneous distribution of discrete gold nanoparticles and negligible agglomeration. This morphology can be credited to the efficiency of the extract applied to grow the nanostructures. The histogram of SEM has been shown in Fig. 2D which was obtained by digital analysis. It consisted of size analysis of more than 200 Au NS representing almost 75% of particle size distribution. The size was found to be 2-5 nm ± 1.2 nm and rest of them exist in the range of 5-10 nm.

Many important features can be expected out of the morphology of hybrid; namely, this structure ensures ultra-high conductivity, firstly due to graphene itself, secondly owing to the presence of metallic nanostructures. Therefore, the final product endows a unique interconnected network, which provides a great potential for its use in electrical applications. The electrical

conductivity of this graphene based hybrid strongly relies on the capacity of electrons percolation between the individual graphene sheets. The metallic interconnected sheets allow the fast electron movement through the seamlessly high surface 3D network. This may lead to sensitive electrocatalysis. Furthermore, overall 3D morphology serves as an enhanced electrochemical substrate, offering a greater surface area for the interface binding and convenient diffusion to facilitate the electrochemical performance.

The presence of the gold nanostructures on the 2D sheet of graphene was further validated by TEM images as shown in Fig. 2(E-G). These images confirm the ability of our method to achieve a uniform distribution of 2-8 nm diameters gold nanostructures anchored on the graphene nanosheets. Moreover, the corrugated nature of the graphene sheets is also apparent from this analysis. Fig. 1H shows the histograms of TEM, obtained by selecting more than 200 Au NS. It represents almost 75% of particle size distribution with the dimension of 2-4 nm ± 1.2 nm and the rest of them exist in 4-8 nm range. Microscopy results obtained by SEM and TEM are in good agreement and established the novel morphology of our designed hybrid.

The size and structure of the hybrid werefurtherexamined by atomic force microscope (AFM). The representative topographs are shown in Fig. 3. The thickness of the GO stuctures was found to be 100-200 nm (Fig. 3A). However, AFM image of the as-synthesized hybrid revealed the presence of 5-10 nm Au NS spread over the sheet of graphene (Fig. 3B). The respective cross-section analysis of Fig. 3A and 3B show that the average thickness of graphene (Fig. 3A; side panel) decrease from 200 nm to 30 nm (Fig. 3B; side panel). This data indicates the flattening of sheets has occurred in the formation of this hybrid [1].

Optical characteristics were studied by investigating UV-Vis profiles from 200 to 800 nm (Fig. 3C). It can be seen that in the case of the hybrid the spectra exhibited a broad absorption band with blunt apex at 400 nm. Typically, graphene shows absorption at 270 nm, a characteristic of π-conjugation network [36]. However, the red shift in the case of hybrid can be attributed to the less conjugated system, which in turn confirmed that amine molecules are absorbed on the surface supporting the growth of nanostructures. Comparing with the absorption profile of control gold nanostructures which executed λ_{max} of 520 nm, further confirmed the formation of 3D Au NS@GO hybrid.

FTIR analysis was performed to investigate the change in chemical functionalities during the formation of 3D Au NS@GO hybrid. As reported earlier, GO contains carbonyl, epoxy, and hydroxyl groups [37]. Fig. 3D (yellow line) shows these characteristic bands, namely, carbonyl groups in graphene oxide at 1532 cm^{-1} (C=O stretching) and an epoxy group (C-O vibration) emerged at 1095 cm^{-1}. The stretching vibration bands appeared at 3336 cm^{1} was ascribed to O-H and N-H groups. This indicates the presence of amine functionalization of graphene. On the other hand, bending vibration bands obtained at 1570 cm^{-1} were credited to the presence of C=C functionalities. Two important bands appeared at 2931 cm^{-1} and 2850 cm^{-1} owing to the C-H asymmetric and symmetric vibrations, respectively. After the growth reaction of Au NS deposition on the graphene (purple line), the characteristic bands of carbonyl, amine, and oxide groups disappeared suggesting these functionalities have been consumed by Au ions during the synthesis process. This in turn confirms the anchoring of gold nanostructures on the surface of graphene.

The zeta potential of the hybrid was investigated to describe the stability of the materials and their potential to bind the analyte. Graphene functionalized with the amine group showed a

zeta potential of -48 mV (Fig. 3E). The high amount of negative surface charge shows the appropriateness of the surface to host the positive gold ions of the precursor. It is established that the high packing of carbon nanotubes by functionalities increases its dispersion and decrease the direct agglomeration of nanostructures on the scaffolds [34]. If the same model is applied to graphene then strong negative potential of graphene indicates its high dispersability and capability to gather more ions for the nucleation and growth of nanostructures. A zeta potential of 55 mV was obtained in the case of hybrid demonstrating the successful growth of metallic structure on the graphene skeleton and its potential for the immobilization/binding of the negatively charged analytes. The surface potential contributed to the stability of the formed hybrid making it a very promising support for the efficient electrocatalysis of biomolecules [34].

3.2 Basic sensor signals

The electrochemical properties of the fabricated 3D AuNS@GO hybrid were investigated by the cyclic voltammetry technique. Fig. 4 shows representative CV signals of bare glassy carbon electrode (A), Au NS (B), GO (C), and 3D Au NS@GO hybrid (D) when these materials were challenged with 0.3 μM uric acid (UA). Overall, the CV responses of control materials were found insignificant indicating poor transfer of the electrons across the interface of the designed materials (Fig. 4; (A-C)). Among these, in the case of Au NS (Fig. 4B) the oxidation peak appeared (6.0 ± 0.2 μA) at 0.4 V *vs.* Ag/AgCl, due to the inherent metallic and conducting nature of gold depicting electrochemical activity as compared to the bare GCE (Fig. 4A). On the other hand, if the CV response of graphene is observed (Fig. 4C), a broad signal can be seen due to the high amount of non-Faradic current, yet the catalytic activity did not appear towards the presence of UA. However, when the designed 3D Au NS@GO hybrid was used (Fig. 4D), a

prominent, high current intensity peak (18.1 ± 0.1 μA) was obtained. This signal reflected both the conducting nature of graphene and the metallic character of gold. Therefore, this effect can be featured to the synergy characteristics of GO and Au NS; and three-dimensional morphology which gives a large electroactive surface. Importantly, it can be seen that the anodic (410 mV *vs.* Ag/AgCl) and cathodic (200 mV *vs.* Ag/AgCl) peak potential difference was found to be 210 mV. This peak separation validates outstandingly high conductance and fast material kinetics. Furthermore, the precise fine shape of the signal proposes a dense electronic surrounding that produces faradic current. The electrochemical oxidation occurred at low potential (0.41 V *vs.* Ag/AgCl) signifies the strong electrocatalytic capability of the hybrid. This remarkable sensor response of the designed hybrid can be attributed to the conducting nature of graphene, metallic nature of gold nanostructures and quantum effects of their nano-regimen. The Au NS act as the electrical contact between the sheets of graphene in two ways; firstly, by providing an unrestricted flow of the electrons throughout the materials generating high current, and secondly, their presence creates a high surface area for the attachment of analyte, which in turn means a higher number of binding centres. These results strongly advocate the potential of hybrid towards the electrochemical detection of the other essential biomolecules.

3.3 Analytical investigation

The CV responses of the prepared hybrid were also quantified against varying concentrations of UA. In this context, we selected a wide range from 0.005 to 0.8 μM, and the respective signals are shown in Fig. 4E. Clearly, it can be seen that the peak current is gradually increased from 6.8 ± 0.2 μA to 55.2 ± 0.7 μA (linear regression r = 0.986) when challenged with

different concentrations of UA. The important analytical parameters which qualify sensor practical applications *i.e.* the limit of detection (LoD) and limit of quantification (LoQ) were also calculated to be 30 nM (S/N=3) and 100 nM (S/N=3), respectively. We compared these values with previously published data and the results are compiled in Table 1 [38-45]. Our designed material exhibited ultra-sensitive binding over the wide linear range. This special feature is more pronounced when compared with previously reported materials of the same chemical composition, yield less sensitivity [40-42]. This signifies the success of our synthesis strategy. Certainly, this remarkable lower detection limit can be imputed to the special three-dimensional morphology and synergy of graphene and gold nanostructures. This yielded a larger surface area with a heavy electron atmosphere that promoted the fast electron transfer in the electrochemical analysis.

The kinetic process was also investigated and the reaction was observed with increasing the scan rate from 0.01-1 Vs^{-1}. The resultant CV scans are shown in Fig. 4F. It can be seen that the value of anodic current increased from 8.5 ± 0.2 μA to 50.5 ± 0.4 μA with increasing scan rate. A linear relationship (correlation coefficient 0.99) (inset Fig. 4F) validated the binding of UA to the designed hybrid is a diffusion controlled process. The synthesis process offered the preparation of hybrid without self-aggregation due to the presence of biomolecules in the green extract. This ensured improved electrode coverage, providing a high population of the reactive sites which may have contributed towards better electrode kinetics.

3.4 Reproducibility

Reproducibility or repeatability is a key parameter for determining the real life utility of a sensor. For this purpose, ten sensor samples of the 3D Au NS@GO hybrid were freshly prepared and subjected to 0.3 μM uric acid, under optimum conditions. The response of each individual sensor was calculated as the average of 10 successive scans and the results are summarized in Fig. 5A. It can be observed, that the sensor signals are highly stable and validate the strong anchoring of the Au NS over the graphene sheets, and this feature can be accredited to merit of the green method used. Essentially, during the preparation of hybrid, the presence of the assorted types of the biomolecules in the reaction assembly has contributed towards the stability of the material. Moreover, about 99% repeatability of signals show analytical accuracy, powerfully suggesting that proposed sensor in this study can be successfully utilized for practical purposes.

3.5 Selectivity

Selectivity is the ability to respond to a particular analyte, regardless of the presence of other competing species. The major interfering molecule capable to influence the uric acid analysis is ascorbic acid. It is functionally related compound and can co-exist with uric acid in the biological samples [21]. We monitored the electrochemical responses of the developed hybrid towards both uric acid and ascorbic acid for their selective detection. The selectivity was studied at different concentrations, *i.e.* from 0.001-0.8 μM, and the respective CV scans are depicted in Fig. 5B. For the higher concentration of 0.8 μM, the signals appeared at 0.41 mV and 0.69 mV for UA and AA, respectively, and the peak separation was calculated to be 280 mV. It can be noted that the specificity factor was retained with increasing concentration of both analytes. We consider, this high specificity and catalytic activity of hybrid can be attributed to

the overall 3D morphology and synergistic effects of its constituents, *i.e.* ultra-small nanostructures and 2D graphene sheets. The peak current obtained towards 0.8 µM, each of UA and AA are graphically shown in Fig. 5C. It can be evaluated that the 3D Au NS@GO hybrid showed an appreciable specificity of electrochemical sensing of both biomolecules which further confirms that the designed hybrid is capable of differentiating both biological molecules of similar chemical nature with analytical accuracy which can be used for clinical applications.

4 Conclusion

This is the first study where a green *in-situ* growth method is described to furnish a homogeneous spread of very small sized gold nanostructures over the ripples of graphene oxide sheets to yield three-dimensional morphology. Microscopy confirmed the resulting hybrid consisted of GO sheets of 25-30 nm armoured with Au NS in the range of 2-8 nm. The huge population of Au NS over the surface of GO furnished, outstanding morphology and interesting catalytic properties for the detection of clinically important analyte, such as uric acid. The prepared hybrid proved to be very sensitive towards its presence and was able to detect its concentrations reaching down to 30 nM. These outstanding sensing results show that strategies of biological methods can be used to synthesize hybrid materials which are efficient and stable. The sensor exhibited extraordinary sensor characteristics of selectivity and reliability. It generates a new genre of hybrid materials where different compositions of nanostructures can confer unique morphology and fascinating properties which can be tailored to design useful applications.

Competing interests

There are no competing financial interests declared by the authors.

Acknowledgement

The authors are thankful to the International Foundation for Science (IFS) for financial support under Research Grant no. E-5659. The Organization of Islamic Cooperation's (OIC) Standing Committee on Scientific and Technological Cooperation (COMSTECH) co-funded with project with IFS. Further, a part of this research work was funded by The Higher Education Commission of Pakistan under the Project no. 6116 and 6117.

References

[1] I. Khalil, N. M. Julkapli, W. A. Yehye, W. J. Basirun, S. K.Bhargava, Materials 9 (2016) 406.

[2] C. He, D. Liu, W. Lin, Chem. Rev. 115 (2015) 11079-11108.

[3] G. Maduraiveeran, M. Sasidharan, V. Ganesan, Biosens. Bioelectron. 103 (2017) 113-129.

[4] S. Z. Bajwa, A. Munawar, and W. S. Khan, Pharm. Bioprocess. 5 (2017) 11-15.

[5] M. Hasanzadeh, N. Shadjou, A review. Microchim. Acta. 184 (2017) 389-414.

[6] G. Yang, F. Zhao, Biosens. Bioelectron. 64 (2015) 416-422.

[7] H. Lee, T. K. Choi, Y. B. figLee, H. R. Cho, R. Ghaffari, L. Wang, H. J. Choi, T. D. Chung, N. Lu, T. Hyeon, Nat. Nanotechnol. 11 (2016) 566.

[8] S. G. Chatterjee, S. Chatterjee, A. K. Ray, A. K. Chakraborty, A review. Sens. Actuators B 221 (2015) 1170-1181.

[9] B. Y. Wu, S. H. Hou, F. Yin, Z. X. Zhao, Y. Y. Wang, X. S. Wang, Q. Chen, Biosens. Bioelectron. 22 (2007) 2854-2860.

[10] P. Pananon, C. Sriprachuabwong, A.Wisitsoraat, P. Chuysinuan, A. Tuantranont, P. Saparpakorn, D. Dechtrirat, RSC Adv. 8 (2018) 12724-12732.

[11] B. Dang, Y. Chen, H. Wang, B. Chen, C. Jin, Q. Sun, Nanomaterials 8 (2018) 52.

[12] A. Karmakar, T. Mallick, S. Das, N. A. Begum, Nano-Structures & Nano-Objects 13 (2018) 1-20.

[13] J. Phiri, L. S. Johansson, P. Gane, T. C. Maloney, Nanoscale 10 (2018) 9569-9582.

[14] J. Li, D. Kuang, Y. Feng, F. Zhang, Z. Xu, M. Liu, D. Wang, Biosens. Bioelectron. 42 (2013) 198-206.

[15] H. Duan, D. Wang, Y. Li, Chem. Soc. Rev. 44 (2015) 5778-5792.

[16] S. Francis, S. Joseph, E. P. Koshy, B. Mathew, Environ. Sci. Pollut. Res. 24 (2017) 17347-17357.

[17] D. H. Jo, J. H. Kim, T. G. Lee, J. H. Kim, Nanomed. Nanotech. Biol. Medicine 11 (2015) 1603-1611.

[18] C. Gonnelli, C. Giordano, U. Fontani, M.C. Salvatici, S. Ristori, Adv. Bionanomat. (2018) 155-164.

[19] F. Jiang, R. Yue, Y. Du, J. Xu, P Yang, Biosens. Bioelectron. 44 (2013) 127-131.

[20] I. A. Abdelhakim, A. M. Abdel-baky, D. W. Bishay, J. Pharmacogn. Phytochem.6 (2017) 2559-2562.

[21] Q. Zhu, J. Bao, D. Huo, M. Yang, H. Wu, C. Hou, Y. Zhao, X. Luo, H Fa, J. Electroanal. Chem. 99 (2017) 459-467.

[22] N. Nakanishi, M. Okamoto, H. Yoshida, Y. Matsuo, K. Suzuki, K. Tatara, Eur. J. Epidemiol. 18 (2003) 523-530.

[23] N. J. Pagidipati, C. N. Hess, R. M. Clare, A. Akerblom, P. Tricoci, D. Wojdyla, R. T. Keenan, S. James, C. Held, K. W. Mahaffey, Am. Heart J. 187 (2017) 53-61.

[24] T. V. Fiorentino, F. Sesti, E. Succurro, E. Pedace, F. Andreozzi, A. Sciacqua, M. L. Hribal, F. Perticone, G. Sesti, Acta Diabetol. 8 (2018) 835–842.

[25] J. R. Venugopal, S. Ramakrishna, Fut. Medicine 11 (2016) 1511-1513.

[26] X. Liu, P. Lin, X. Yan, Z. Kang, Y. Zhao, Y. Lei, C. Li, H. Du, Y. Zhang, Sens. Actuators B 176 (2013) 22-27.

[27] D. Kim, Q. Wei, D. H. Kim, D. Tseng, J. Zhang, E. Pan, O. Garner, A. Ozcan, D. Di. Carlo, Anal. Chem. 90 (2017) 690-695.

[28] L. Cui, J. Liu, X. Yan, S. Hu, Anal. Chem. 89 (2017) 11737-11743.

[29] L. Syedmoradi, M. Daneshpour, M. Alvandipour, F. A. Gomez, H. Hajghassem, K. Omidfar, Biosens. Bioelectron. 87 (2017) 373-387.

[30] A. Malapert, V. Tomao, O. Dangles, E. Reboul, J. Agri. Food. Chem. 66 (2018) 4614-4620.

[31] A. Bulavchenko, A. Arymbaeva, V. Tatarchuk, Russ. J. Phys. Chem. A 82 (2015) 801-806.

[32] V. Borodina, Y. A. Mirgorod, Kinet. Catal. 55 (2014) 683-687.

[33] C. Díaz, M. Valenzuela, M. Laguna-Bercero, A. Orera, D. Bobadilla, S. Abarca, O. Peña, RSC Adv. 7 (2017) 27729-27736.

[34] A. Munawar, M. A. Tahir, A. Shaheen, P. A. Lieberzeit, W. S. Khan, and S. Z. Bajwa, J. Hazard. Mater. 342 (2018) 96-106.

[35] S. Sharma, N. Singh, V. Tomar, and R. Chandra, Biosens. Bioelectron. 107 (2018) 76-93.

[36] S. Saxena, T. A. Tyson, S. Shukla, E. Negusse, H. Chen, J. Bai, Appl. Phys. Lett. 99 (2011) 013104.

[37] Y. Hu, K. Wang, Q. Zhang, F. Li, T. Wu, L. Niu, Biomatateriales 33 (2016) 1097-1106.

[38] X. Gao, R. Gui, K.Q. Xu, H. Guo, H. Jin, Z. Wang, N. J. Chem. 42 (2018) 14796-14804.

[39] L. Yang, D. Liu, J. Huang, T. You, Sens. Actuators B 193 (2014) 166-172.

[40] X. Tian, C. Cheng, H. Yuan, J. Du, D. Xiao, S. Xie, M. M. Choi, Talanta 93 (2012) 79-85.

[41] C. Wang, J. Du, H. Wang, C. Zou, F. Jiang, P. Yang, Y. Du, Sens. Actuators B 204 (2014) 302-309.

[42] D. Han, T. Han, C. Shan, A. Ivaska, L. Niu, Electroanal. 22 (2010) 2001-2008.

[43] S. Wang, W. Zhang, X. Zhong, Y. Chai, R. Yuan, Anal. Methods 7 (2015) 1471-1477.

[44] M. Liu, Q. Chen, C. Lai, Y. Zhang, J. Deng, H. Li, S. Yao, Biosens. Bioelectron. 48 (2013) 75-81.

List of Figures

Fig. 4 Sensor parameters: Cyclic voltammetry responses of bare, Au NS, GO, and 3D Au NS@GO hybrid with modified electrode at 0.3 µM uric acid background electrolyte NaH_2PO_4. H_2O (50 mM), scan rate of 50 mVs^{-1}. (A) CV responses of bare, (B) Au Ns, (C) GO (D) 3D Au NS@GO hybrid; (E) CVs of 3D Au NS@GO hybrid for different concentrations of uric acid (0.005-0.8 µM) with background electrolyte NaH_2PO_4. H_2O (50 mM), scan rate of 50 mVs^{-1}. Inset shows a linear regression plot of the anodic current against different concentrations of uric acid; (F) CVs of 3D Au NS@GO hybrid against 0.8 µM at different scan rate; inset shows a linear relation plot; experimental conditions are with background electrolyte NaH_2PO_4. H_2O (50 mM),, scan range 0.1-1 Vs^{-1}. The potential values refer to a Ag/AgCl reference electrode.

Fig. 5 Reproducibility and selectivity profile: (A) reproducibility profile of electrochemical responses towards 0.3 µM uric acid, NaH_2PO_4. H_2O (50 mM) at scan rate 50 mVs^{-1}; (B) CV responses of 3D Au NS@GO hybrid modified GCE for different concentrations of both UA and AA (0.001-0.8 µM); (C) Graphical depiction of the comparison of the uric acid response with most interfering agent ascorbic acid on the 3D Au NS@GO hybrid modified GCE.

Graphical Abstract

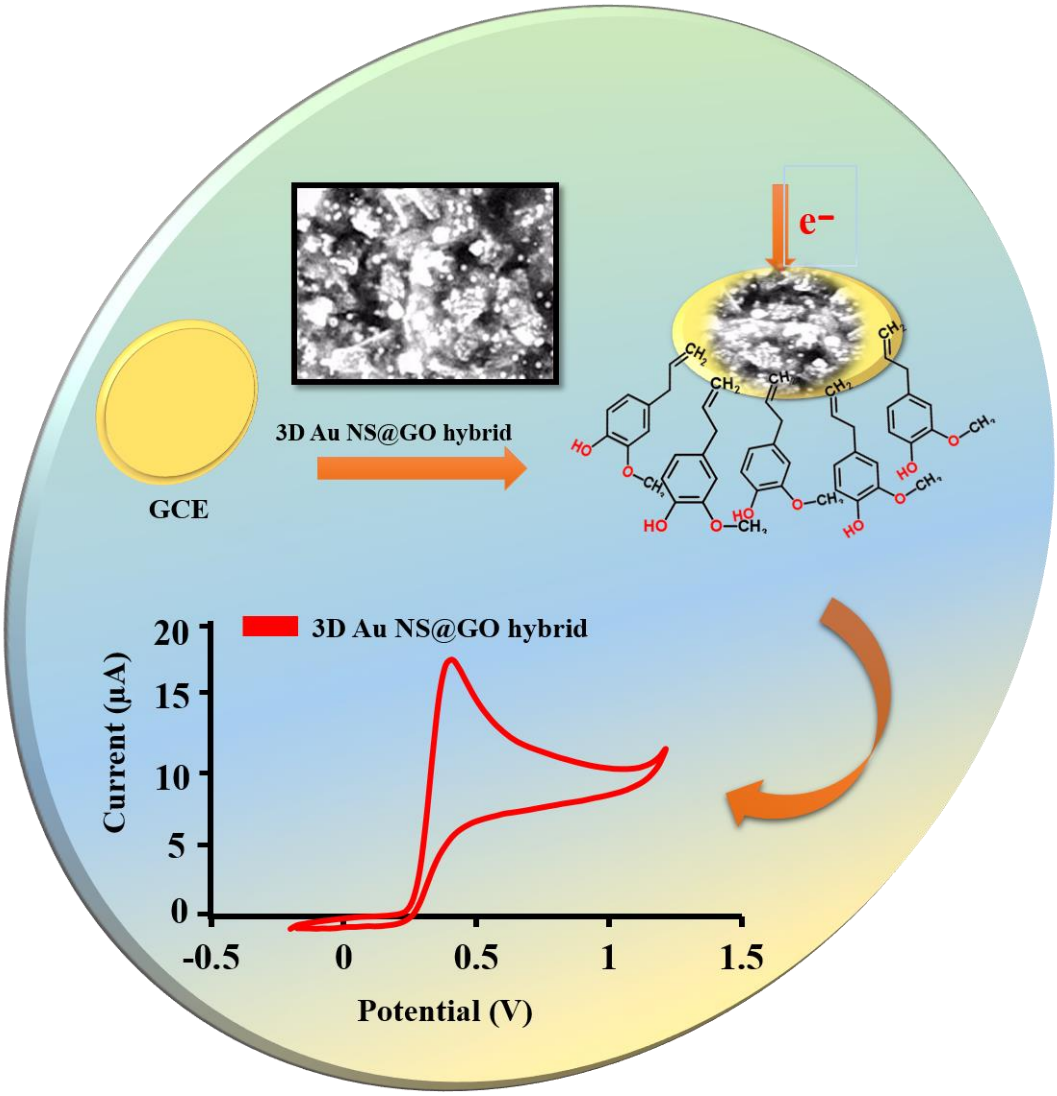

Fig. 1

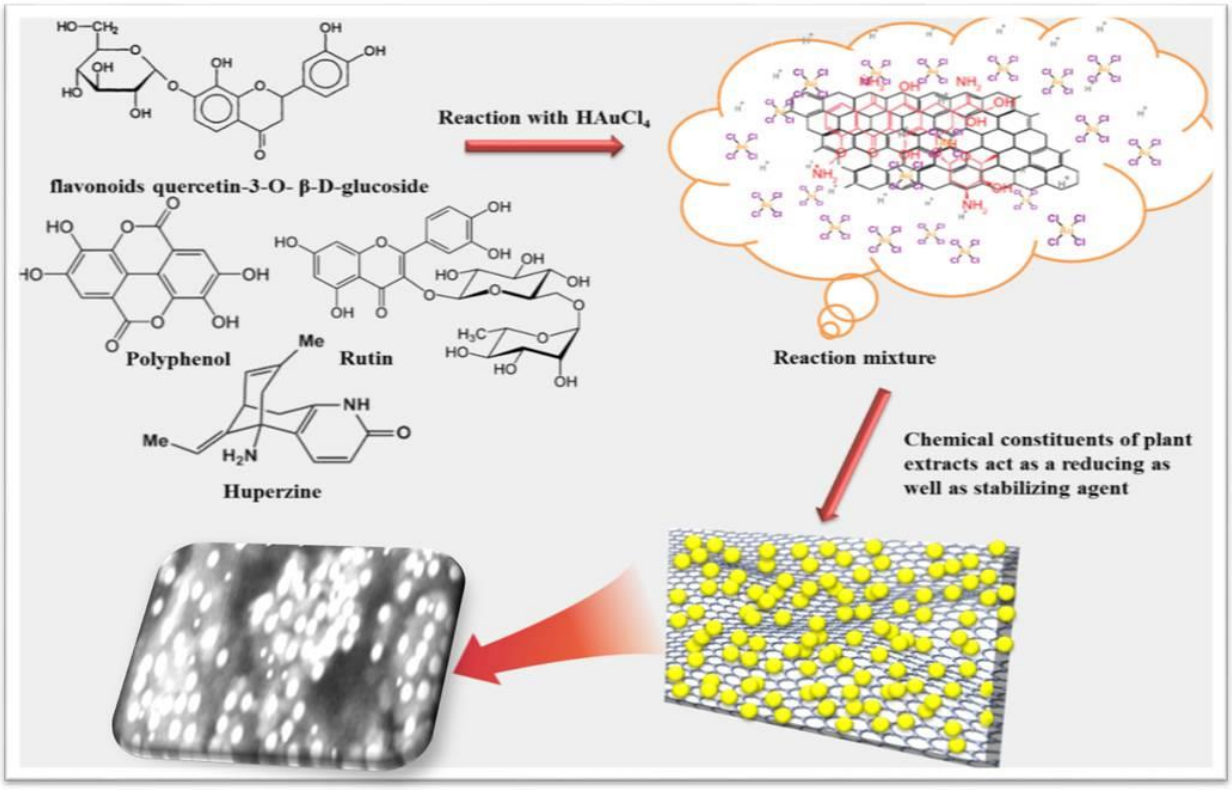
Reaction with $HAuCl_4$
flavonoids quercetin-3-O- β-D-glucoside
Polyphenol
Rutin
Huperzine
Reaction mixture
Chemical constituents of plant extracts act as a reducing as well as stabilizing agent

Fig. 2

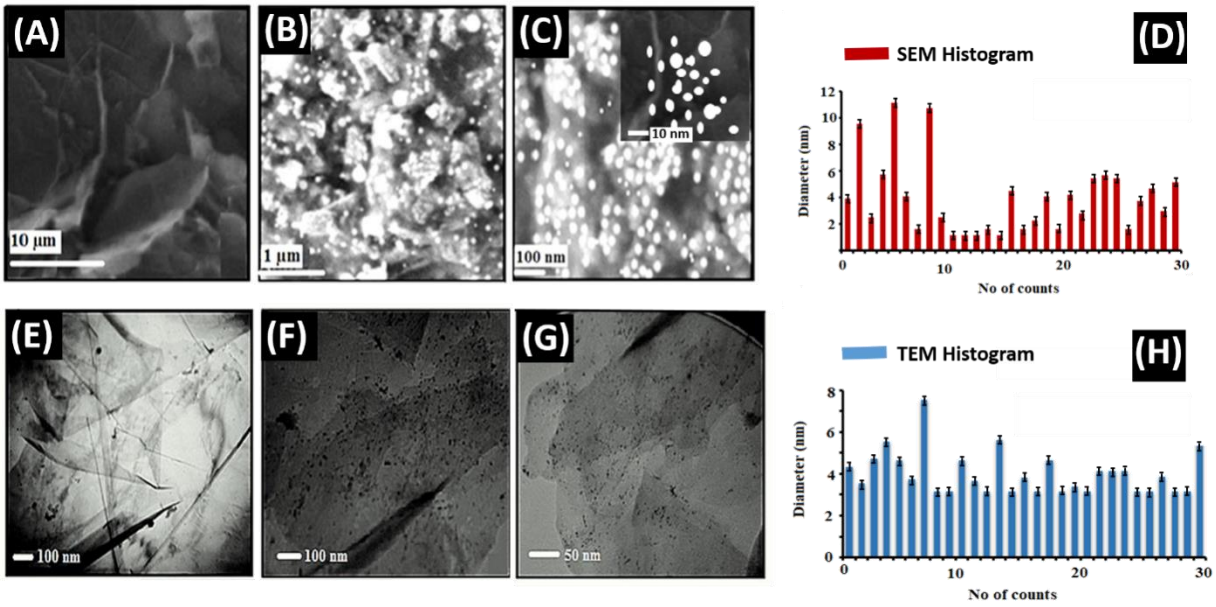
(A)
10 µm
(B)
1 µm
(C)
10 nm
100 nm
(D)
SEM Histogram
Diameter (nm)
No of counts
(E)
100 nm
(F)
100 nm
(G)
50 nm
(H)
TEM Histogram
Diameter (nm)
No of counts

Fig. 3

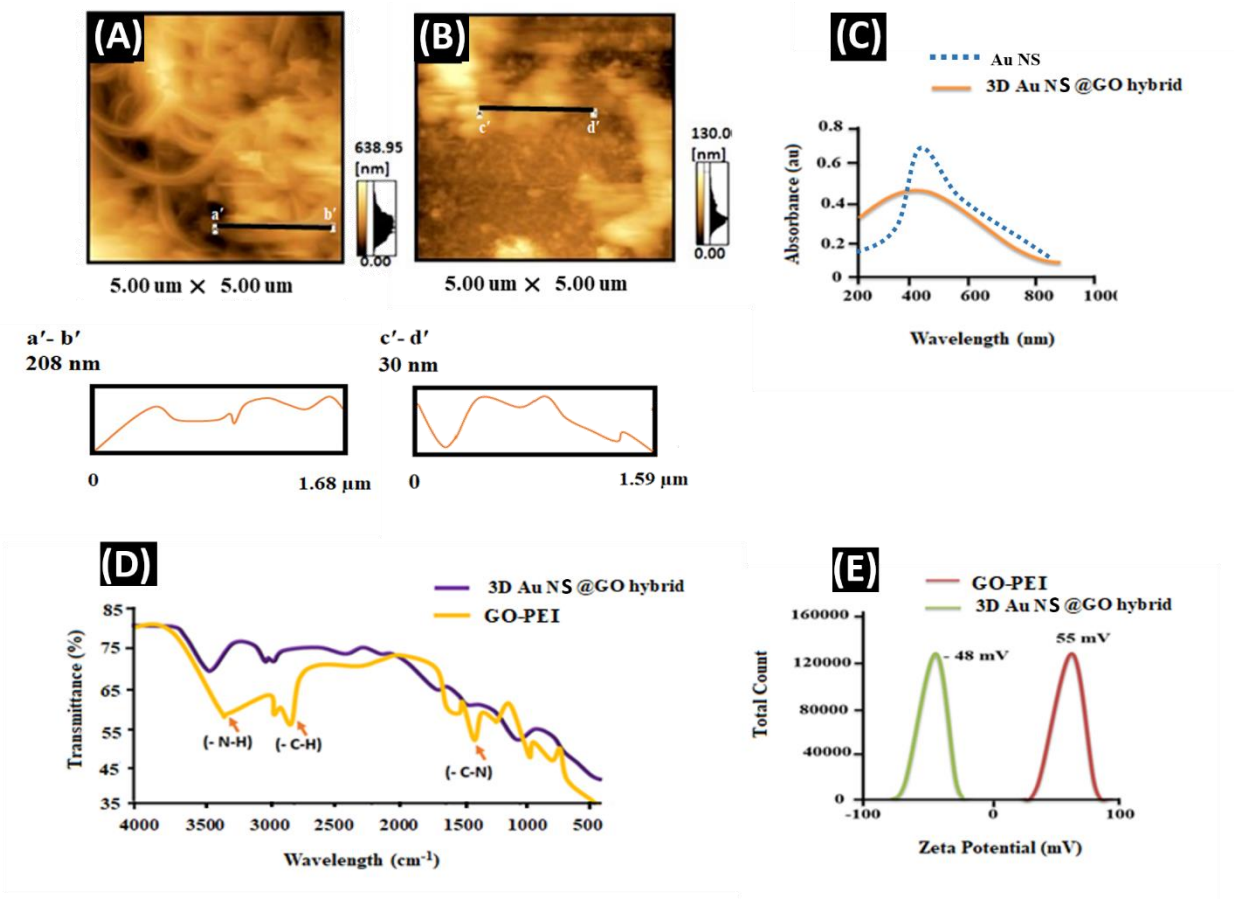
(A)
638.95
[nm]
0.00
a′
b′
5.00 um × 5.00 um
(B)
130.0
[nm]
0.00
c′
d′
5.00 um × 5.00 um
a′- b′
208 nm
0
1.68 µm
c′- d′
30 nm
0
1.59 µm
(C)
Au NS
3D Au NS @GO hybrid
Absorbance (au)
0.8
0.6
0.4
0.2
0
200
400
600
800
Wavelength (nm)
(D)
3D Au NS @GO hybrid
GO-PEI
Transmittance (%)
85
75
65
55
45
35
(- N-H)
(- C-H)
(- C-N)
4000
3500
3000
2500
2000
1500
1000
500
Wavelength (cm-1)
(E)
GO-PEI
3D Au NS @GO hybrid
Total Count
160000
120000
80000
40000
0
- 48 mV
55 mV
-100
0
100
Zeta Potential (mV)

Fig. 4

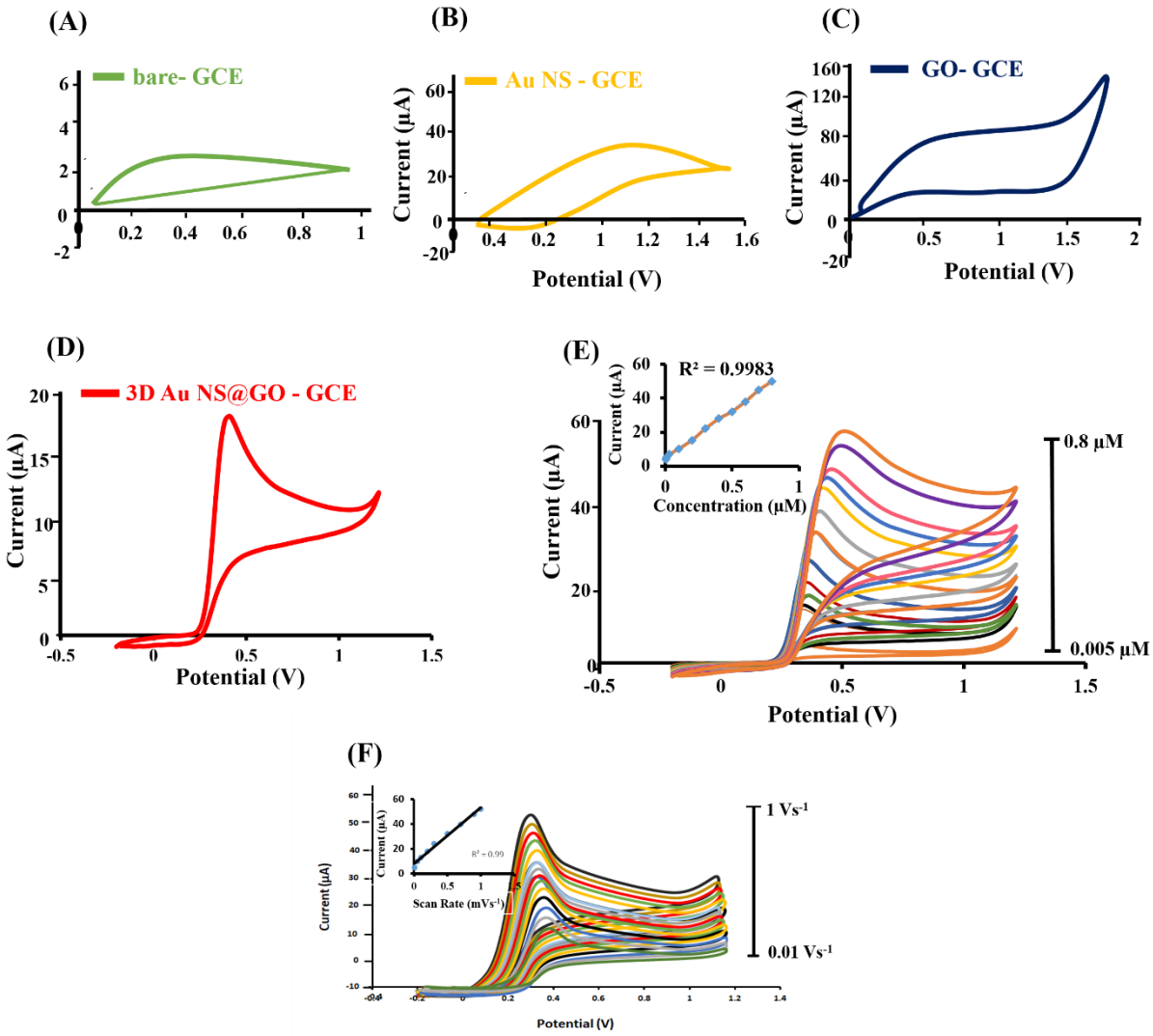
(A)
bare- GCE
(B)
Au NS - GCE
Current (µA)
Potential (V)
(C)
GO- GCE
Current (µA)
Potential (V)
(D)
3D Au NS@GO - GCE
Current (µA)
Potential (V)
(E)
R² = 0.9983
Current (µA)
Concentration (µM)
0.8 µM
0.005 µM
Current (µA)
Potential (V)
(F)
Current (µA)
Scan Rate (mVs⁻¹)
1 Vs⁻¹
0.01 Vs⁻¹
Potential (V)

Fig. 5

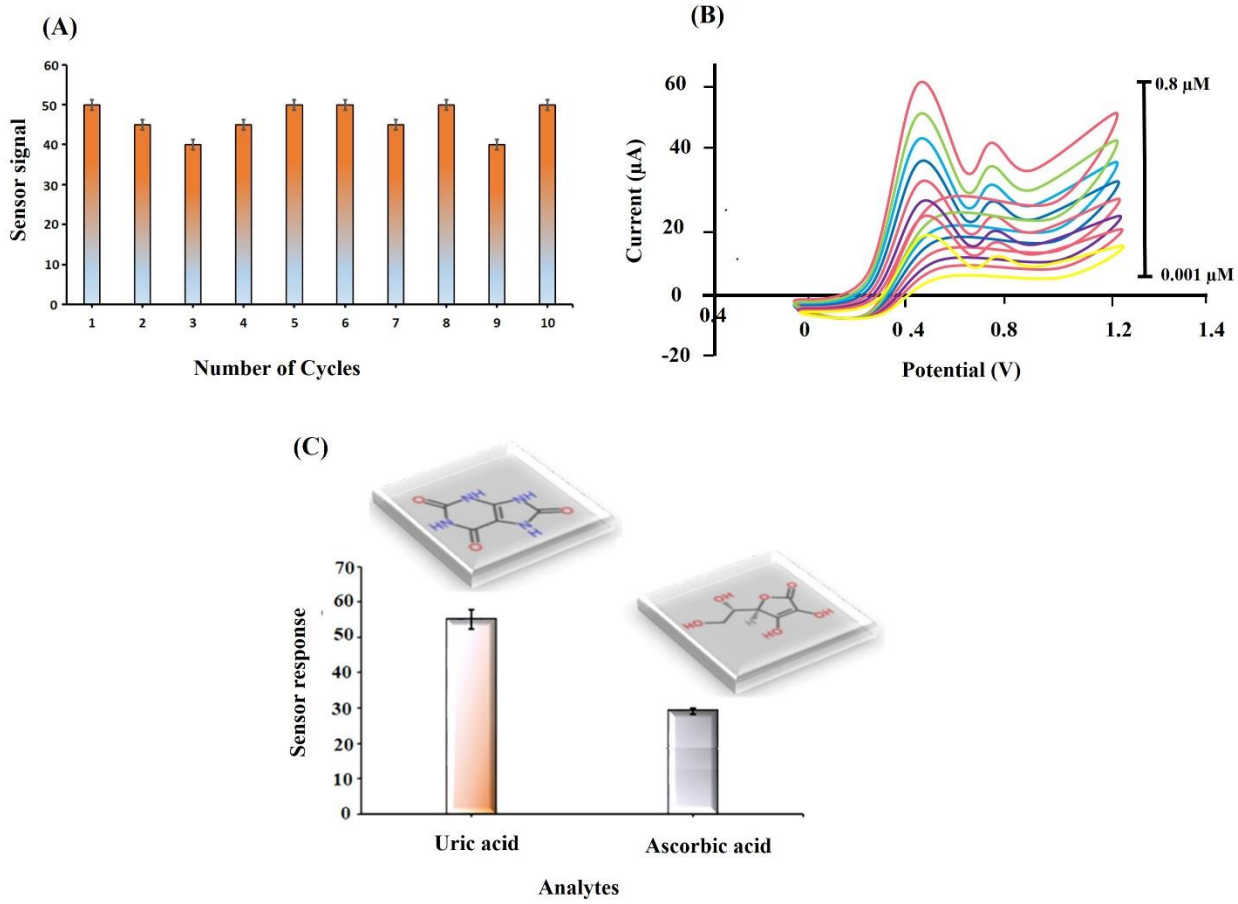
(A)
Sensor signal
Number of Cycles
(B)
Current (µA)
Potential (V)
0.8 µM
0.001 µM
(C)
Sensor response
Uric acid
Ascorbic acid
Analytes

List of Table

Table 1.

Material	Linear Range (μM)	Detection Limit (nM)	Reference
Au–Ag NPs/GO/TH	1-100	300	[38]
ERGO	0.5-60	500	[39]
AuNPs–β-CD–Gra	0.5–60	1800	[40]
Au/RGO/GCE	8.8-530	1500	[41]
CTAB-GO/MWNT/GCE	3.0–60	1.5	[39]
Chitosan-graphene	2.0–45	2000	[42]
RGO–PAMAM–MWCNT–AuNPs	20-1800	300	[43]
Fe_3O_4@Au-S-Fc/GS-chitosan	1-300	200	[44]
Au NS@GO hybrid	**0.005-0.8**	**30**	**This work**

Supplementary Information

SI. 1

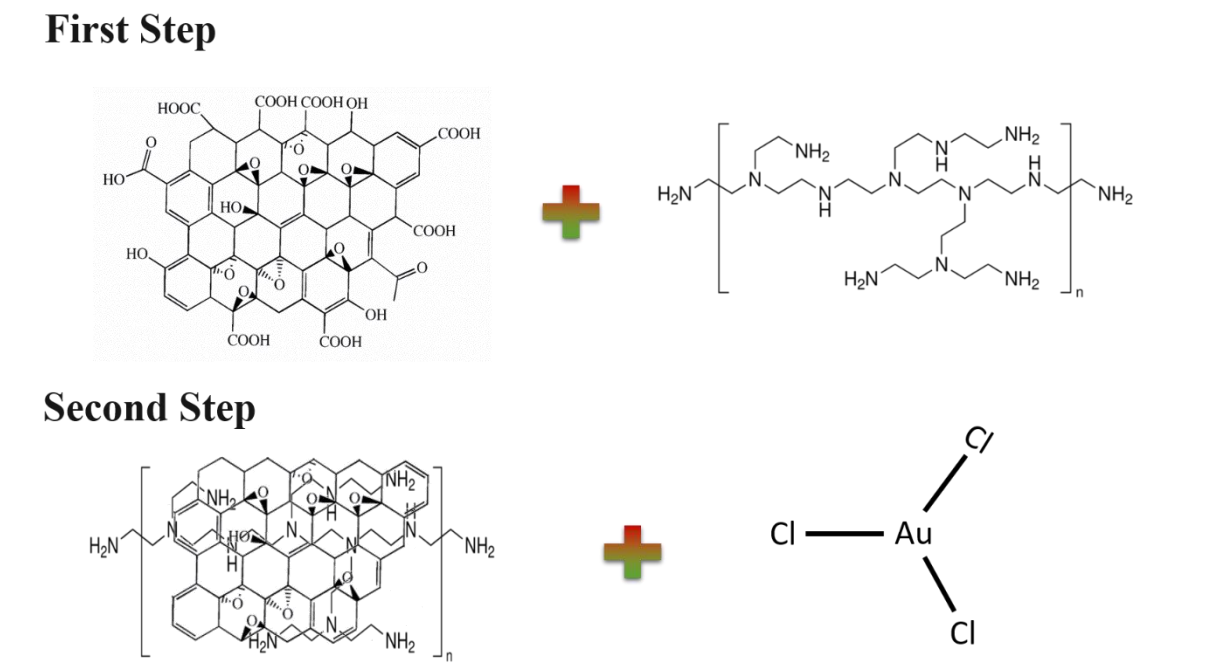

SI. 1 Step-wise representation of the mechanism involved in the synthesis of 3D Au NS@GO hybrid.